

Contribution of the a_1 meson to the axial nucleon-to-delta transition form factors

Y. Ünal,¹ A. Küçükarslan,¹ and S. Scherer²

¹*Physics Department, Çanakkale Onsekiz Mart University, 17100 Çanakkale, Turkey*

²*PRISMA Cluster of Excellence, Institut für Kernphysik,
Johannes Gutenberg-Universität Mainz, D-55099 Mainz, Germany*

(Dated: August 9, 2018)

Abstract

We analyze the low- Q^2 behavior of the axial form factor $G_A(Q^2)$, the induced pseudoscalar form factor $G_P(Q^2)$, and the axial nucleon-to-delta transition form factors $C_5^A(Q^2)$ and $C_6^A(Q^2)$. Building on the results of chiral perturbation theory, we first discuss $G_A(Q^2)$ in a chiral effective-Lagrangian model including the a_1 meson and determine the relevant coupling parameters from a fit to experimental data. With this information, the form factor $G_P(Q^2)$ can be predicted. For the determination of the transition form factor $C_5^A(Q^2)$, we make use of an SU(6) spin-flavor quark-model relation to fix two coupling constants such that only one free parameter is left. Finally, the transition form factor $C_6^A(Q^2)$ can be predicted in terms of $G_P(Q^2)$, the mean-square axial radius $\langle r_A^2 \rangle$, and the mean-square axial nucleon-to-delta transition radius $\langle r_{AN\Delta}^2 \rangle$.

I. INTRODUCTION

At the fundamental level, the electroweak form factors of hadrons originate from the dynamics of the constituents of quantum chromodynamics (QCD), namely, quarks and gluons. While a wealth of precision data exists for the electromagnetic form factors of the proton and, to a lesser extent, of the neutron (see, e.g., Refs. [1, 2] for a review), the nucleon form factors of the isovector axial-vector current, the axial form factor G_A and, in particular, the induced pseudoscalar form factor G_P , are not as well known (see, e.g., Refs. [3, 4] for a review). A similar situation occurs in the case of the nucleon-to-delta transition form factors. A considerable amount of data is available for the electromagnetic transition form factors (see, e.g., Refs. [5, 6] for a review), whereas very little is known about the axial nucleon-to-delta transition form factors [7–11]. On the theoretical side, there have been various approaches to determining the nucleon-to-delta transition form factors. Calculations have been performed in the framework of quark models [12–16], chiral effective field theory [17–19], lattice QCD [20–22], and light-cone QCD sum rules [23, 24]. Moreover, a substantial amount of work has been devoted to the question of how to parametrize and extract the form factors from experimental data [25–34].

In this article, based on the results of Ref. [35], we make use of a semiphenomenological description of the nucleon axial form factor G_A and the induced pseudoscalar form factor G_P to predict, using certain model assumptions, two of the four axial nucleon-to-delta transition form factors, namely, C_5^A and C_6^A . We will assume that the exchange of the axial-vector meson $a_1(1260)$ provides a dominant contribution to the form factor C_5^A at low values of Q^2 . Such a scenario was already envisaged decades ago in Ref. [36], where the common use of a dipole form was questioned.

II. AXIAL-VECTOR CURRENT OPERATOR IN QCD

In terms of the up-quark and down-quark fields,

$$q(x) = \begin{pmatrix} u(x) \\ d(x) \end{pmatrix},$$

the Cartesian components of the isovector axial-vector current operator are defined as

$$A_j^\mu(x) = \bar{q}(x)\gamma^\mu\gamma_5\frac{\tau_j}{2}q(x). \quad (1)$$

In the isospin-symmetric limit, $m_u = m_d = \hat{m}$, the divergence of the isovector axial-vector current is given by

$$\partial_\mu A_j^\mu = i\hat{m}\bar{q}\gamma_5\tau_jq \equiv \hat{m}P_j, \quad (2)$$

where P_j is the j th component of the pseudoscalar quark density. After coupling external c-number axial-vector fields $a_{\mu j}(x)$ to the axial-vector current operators $A_j^\mu(x)$ [37],

$$\mathcal{L}_{\text{ext}} = \sum_{j=1}^3 a_{\mu j}(x)A_j^\mu(x), \quad (3)$$

the invariant amplitude for a transition from a hadronic state $|A(p_i)\rangle$ to $|B(p_f)\rangle$, induced by a plane-wave external field of the form $a_{\mu j}(x) = \epsilon_{\mu j}(q)e^{-iq\cdot x}$, is defined as (no summation

over j implied)

$$\mathcal{M} = i\epsilon_{\mu j}(q)\langle B(p_f)|A_j^\mu(0)|A(p_i)\rangle, \quad (4)$$

where four-momentum conservation $p_f = p_i + q$ due to translational invariance is implied.

III. PARAMETRIZATION OF THE NUCLEON-TO-NUCLEON AND NUCLEON-TO- Δ TRANSITIONS

The axial-vector current matrix element between nucleon states can be parametrized as [35]

$$\langle N(p_f, s_f)|A_j^\mu(0)|N(p_i, s_i)\rangle = \bar{u}(p_f, s_f) \left[\gamma^\mu \gamma_5 G_A(Q^2) + \frac{q^\mu}{2m_N} \gamma_5 G_P(Q^2) \right] \frac{\tau_j}{2} u(p_i, s_i), \quad (5)$$

where $q = p_f - p_i$, $Q^2 = -q^2$, and m_N is the nucleon mass. The Pauli matrix τ_j has to be evaluated between nucleon isospinors. At $Q^2 = 0$, the axial form factor reduces to the axial-vector coupling constant $g_A = 1.2723 \pm 0.0023$ [38]. At $Q^2 = m_\mu^2$, where m_μ is the muon mass, the induced pseudoscalar coupling constant is defined as

$$g_p = \frac{m_\mu}{2m_N} G_P(m_\mu^2). \quad (6)$$

Recently, the MuCap Collaboration obtained $g_p = 8.06 \pm 0.55$ [39], which is in very good agreement with the result of chiral perturbation theory [40, 41], $g_p = 8.26 \pm 0.23$ [3].¹

Introducing the spherical tensor notation [42],

$$A_{\pm 1}^{\mu(1)} = \mp \frac{1}{\sqrt{2}} (A_1^\mu \pm iA_2^\mu), \quad A_0^{\mu(1)} = A_3^\mu,$$

and using isospin symmetry, we express the matrix element of the spherical isospin components ($\alpha = +1, 0, -1$) between a nucleon state and a Δ state as

$$\langle 3/2, \tau_\Delta | A_\alpha^{\mu(1)} | 1/2, \tau \rangle = (1/2, \tau; 1, \alpha | 3/2, \tau_\Delta) \langle 3/2 || A^{\mu(1)} || 1/2 \rangle, \quad (7)$$

where $\langle 3/2 || A^{\mu(1)} || 1/2 \rangle$ denotes the reduced matrix element and $(1/2, \tau; 1, \alpha | 3/2, \tau_\Delta)$ is the relevant Clebsch-Gordan coefficient. For example, using $\langle 1/2, 1/2; 1, 0 | 3/2, 1/2 \rangle = \sqrt{2/3}$, we obtain the reduced matrix element in terms of the p to Δ^+ transition as

$$\langle 3/2 || A^{\mu(1)} || 1/2 \rangle = \sqrt{\frac{3}{2}} \langle \Delta^+ | A_0^{\mu(1)} | p \rangle. \quad (8)$$

Because of its very short lifetime of the order of 10^{-23} s, the Δ is not a stable one-particle state. It shows up as a pole of the S -matrix in the complex-energy plane and a model-independent definition of its properties should take place at a complex squared four-momentum $s = p^2 = z_\Delta^2$ with a complex pole position $z_\Delta = m_\Delta - i\Gamma_\Delta/2$ [43]. From the experimental side, this means that one needs to look for a process which involves the transition to an intermediate Δ comprising, as a building block, the "matrix element" one

¹ The result of older experiments has been somewhat under debate (see Table II of Ref. [4]) with a world average of $g_p = 10.5 \pm 1.8$ of all ordinary muon capture experiments.

is interested in. For example, weak single-pion production in the Δ -resonance region [25], $\nu N \rightarrow \ell N \pi$, contains information on both the vector and axial-vector nucleon-to-delta transitions. While experiments are performed for real values of the squared center-of-mass energy s , an analytic continuation of the three-point function to complex values allows for an extraction of the delta properties from the theoretical side. In Ref. [43], a method applicable for spin-1/2 resonances was proposed to extract from the general vertex only that piece surviving as the residue at the pole. In the vicinity of the pole, the renormalized dressed propagator of the resonance is written as²

$$S(p) = \frac{1}{\not{p} - z} + \text{n.p.} = \frac{\not{p} + z}{p^2 - z^2} + \text{n.p.} = \sum_{i=1}^2 \frac{w^i(p)\bar{w}^i(p)}{p^2 - z^2} + \text{n.p.},$$

where n.p. refers to nonpole, i.e. regular terms and w^i, \bar{w}^i are Dirac spinors with complex masses z . An external leg of the Green function is multiplied by $p^2 - z^2$ and the result is then evaluated between the corresponding Dirac spinors. The generalization to the case of Rarita-Schwinger vector-spinors $\bar{w}_\lambda(p, s)$ [44, 45] with a complex mass z_Δ and $p^2 = z_\Delta^2$ was described in Ref. [46].

Even though a description in terms of stable states does not exist, we use Dirac's bra-ket notation, with the understanding that the relevant amplitude is extracted at the complex pole. The Lorentz structure of the reduced matrix element may be written as

$$\langle \Delta(p_f, s_f) | A^{\mu(1)}(0) | N(p_i, s_i) \rangle = \bar{w}_\lambda(p_f, s_f) \Gamma_A^{\lambda\mu} u(p_i, s_i). \quad (9)$$

Here, the initial nucleon is described by the Dirac spinor $u(p_i, s_i)$ with real mass m_N and $p_i^2 = m_N^2$, the final $\Delta(1232)$ is described via the Rarita-Schwinger vector-spinor $\bar{w}_\lambda(p_f, s_f)$ [44, 45] with a complex mass z_Δ and $p_f^2 = z_\Delta^2$. The explicit form of \bar{w}_λ can be found in Ref. [46] but we will only need the properties of Eq. (11) below.

In the following, it is always understood that the ‘‘tensor’’ $\Gamma_A^{\lambda\mu}$ is evaluated between on-shell spinors u and \bar{w}_λ , satisfying

$$\not{p}_i u(p_i, s_i) = m_N u(p_i, s_i), \quad (10)$$

$$\bar{w}_\lambda(p_f, s_f) \not{p}_f = z_\Delta \bar{w}_\lambda(p_f, s_f), \quad \bar{w}_\lambda(p_f, s_f) \gamma^\lambda = 0, \quad \bar{w}_\lambda(p_f, s_f) p_f^\lambda = 0. \quad (11)$$

The last two equations are responsible for identifying the spin-3/2 component of the Rarita-Schwinger vector-spinor. We tacitly assume that this is also true for the analytic continuation. The ‘‘tensor’’ $\Gamma_A^{\lambda\mu}$ contains a superposition of four Lorentz tensors [25, 26], which we choose to be [19, 21]

$$\Gamma_A^{\lambda\mu} = \frac{C_3^A(Q^2)}{m_N} (g^{\lambda\mu} \not{q} - q^\lambda \gamma^\mu) + \frac{C_4^A(Q^2)}{m_N^2} (g^{\lambda\mu} p_f \cdot q - q^\lambda p_f^\mu) + C_5^A(Q^2) g^{\lambda\mu} + \frac{C_6^A(Q^2)}{m_N^2} q^\lambda q^\mu. \quad (12)$$

In particular, C_5^A and C_6^A correspond to the axial nucleon form factor G_A and the induced pseudoscalar form factor G_P , respectively.

Equations (9)–(12) provide the general framework for an unstable Δ resonance. However, in the present work, we do not calculate any loop corrections to Δ -resonance properties. We therefore also neglect the width Γ_Δ such that our results for the form factors turn out to be real.

² Note that $\not{p} + z = \sum_{i=1}^2 w^i(p)\bar{w}^i(p) + \mathcal{O}(p^2 - z^2)$.

IV. AXIAL-VECTOR COUPLING CONSTANTS IN THE STATIC QUARK MODEL

Here, we recall an SU(6) spin-flavor quark-model relation, which will be applied in the subsequent calculations. In the static quark model, the operator $A_{z,3}$ is given by

$$A_{z,3} = \frac{1}{2} \sum_{i=1}^3 \tau_3(i) \sigma_z(i).$$

The axial-vector coupling constant is obtained as

$$\langle p, S_z = 1/2 | A_{z,3} | p, S_z = 1/2 \rangle = \frac{1}{2} g_A. \quad (13)$$

Inserting the appropriate quark-model wave function,

$$\begin{aligned} |p, S_z = 1/2 \rangle = \frac{1}{\sqrt{18}} [& 2(u \uparrow u \uparrow d \downarrow + u \uparrow d \downarrow u \uparrow + d \downarrow u \uparrow u \uparrow) \\ & - (u \uparrow u \downarrow d \uparrow + u \downarrow u \uparrow d \uparrow + u \uparrow d \uparrow u \downarrow \\ & + d \uparrow u \uparrow u \downarrow + u \downarrow d \uparrow u \uparrow + d \uparrow u \downarrow u \uparrow)], \end{aligned} \quad (14)$$

one obtains

$$g_A = 2 \langle p, S_z = 1/2 | A_{z,3} | p, S_z = 1/2 \rangle = 3 \langle p, S_z = 1/2 | \tau_3(3) \sigma_z(3) | p, S_z = 1/2 \rangle = \frac{5}{3}. \quad (15)$$

On the other hand, evaluating Eq. (5) for $\vec{p}_i = \vec{p}_f = \vec{0}$ and $S_{zi} = S_{zf} = 1/2$ yields

$$\bar{u}^{(1)}(\vec{0}) \gamma^3 \gamma_5 g_A u^{(1)}(\vec{0}) \times \frac{1}{2} = 2m_N \frac{g_A}{2} (1 \ 0 \ 0 \ 0) \begin{pmatrix} 0 & 0 & 1 & 0 \\ 0 & 0 & 0 & -1 \\ -1 & 0 & 0 & 0 \\ 0 & 1 & 0 & 0 \end{pmatrix} \begin{pmatrix} 0 & 0 & 1 & 0 \\ 0 & 0 & 0 & 1 \\ 1 & 0 & 0 & 0 \\ 0 & 1 & 0 & 0 \end{pmatrix} \begin{pmatrix} 1 \\ 0 \\ 0 \\ 0 \end{pmatrix} = 2m_N \frac{g_A}{2}. \quad (16)$$

The factor $2m_N$ originates from our normalization of the Dirac spinors (see Appendix A). When comparing the expression of Eq. (16) to the quark-model result of Eq. (13), we have to discard this factor.

Using

$$\begin{aligned} |\Delta^+, S_z = 1/2 \rangle = \frac{1}{3} (& u \uparrow u \uparrow d \downarrow + u \uparrow d \downarrow u \uparrow + d \downarrow u \uparrow u \uparrow \\ & + u \uparrow u \downarrow d \uparrow + u \downarrow u \uparrow d \uparrow + u \uparrow d \uparrow u \downarrow \\ & + d \uparrow u \uparrow u \downarrow + u \downarrow d \uparrow u \uparrow + d \uparrow u \downarrow u \uparrow) \end{aligned} \quad (17)$$

together with Eq. (14), one obtains for the nucleon-to-delta axial-vector transition

$$\begin{aligned} \langle \Delta^+, S_z = 1/2 | A_{z,3} | p, S_z = 1/2 \rangle &= \frac{3}{2} \langle \Delta^+, S_z = 1/2 | \tau_3(3) \sigma_z(3) | p, S_z = 1/2 \rangle \\ &= \frac{2}{3} \sqrt{2} = \frac{5}{3} \frac{2}{5} \sqrt{2} = \frac{2}{5} \sqrt{2} g_A. \end{aligned} \quad (18)$$

V. CONNECTION TO CHIRAL EFFECTIVE FIELD THEORY

At lowest order in the quark-mass and momentum expansion, the relevant interaction Lagrangian for nucleons reads [47]

$$\mathcal{L}_{\text{int}} = \frac{\mathbf{g}_A}{2} \bar{\Psi} \gamma^\mu \gamma_5 u_\mu \Psi, \quad (19)$$

where \mathbf{g}_A is the chiral limit of the axial-vector coupling constant and

$$\Psi = \begin{pmatrix} p \\ n \end{pmatrix} \quad (20)$$

denotes the nucleon field with two four-component Dirac fields for the proton and the neutron. The so-called chiral vielbein u_μ (see Chap. 4 of Ref. [48] for a detailed discussion) is a traceless, Hermitian, (2×2) matrix,

$$u_\mu = i[u^\dagger(\partial_\mu - ir_\mu)u - u(\partial_\mu - il_\mu)u^\dagger] = \sum_{j=1}^3 \tau_j u_{\mu,j},$$

which involves the external fields $r_\mu = v_\mu + a_\mu$ and $l_\mu = v_\mu - l_\mu$ as well as pions. The latter are contained in the unimodular, unitary, (2×2) matrix u :

$$u(x) = \exp\left(i \frac{\Phi(x)}{2F}\right), \quad (21)$$

$$\Phi(x) = \sum_{j=1}^3 \tau_j \phi_j(x) = \begin{pmatrix} \pi^0(x) & \sqrt{2}\pi^+(x) \\ \sqrt{2}\pi^-(x) & -\pi^0(x) \end{pmatrix},$$

where F denotes the pion-decay constant in the chiral limit: $F_\pi = F[1 + O(\hat{m})] = 92.2 \text{ MeV}$.

The expansion of the chiral vielbein in the pion fields yields

$$u_\mu = 2a_\mu - \frac{\partial_\mu \Phi}{F} + \mathcal{O}(v_\mu \Phi, a_\mu \Phi^2, \partial_\mu \Phi \Phi^2),$$

where

$$a_\mu = \sum_{j=1}^3 \frac{\tau_j}{2} a_{\mu j}.$$

Keeping only the first term of the expansion, i.e., the replacement $u_\mu \rightarrow 2a_\mu$, gives rise to the interaction Lagrangian³

$$\mathcal{L}_{\text{int}} = \sum_{j=1}^3 a_{\mu j} \frac{\mathbf{g}_A}{2} \bar{\Psi} \gamma^\mu \gamma_5 \tau_j \Psi. \quad (22)$$

³ On the other hand, the second term results in the pseudovector pion-nucleon interaction,

$$\mathcal{L}_{\pi NN} = -\frac{\mathbf{g}_A}{2F} \bar{\Psi} \gamma^\mu \gamma_5 \partial_\mu \Phi \Psi.$$

The invariant amplitude for $a_{\mu j}(x) = \epsilon_{\mu j}(q)e^{-iq \cdot x}$, with j fixed, reads

$$\mathcal{M} = i\epsilon_{\mu j}(q)\mathbf{g}_A\bar{u}(p_f)\gamma^\mu\gamma_5\frac{\tau_j}{2}u(p_i).$$

A comparison with Eqs. (4) and (5) yields

$$G_A(Q^2) = \mathbf{g}_A. \quad (23)$$

At lowest order, there is no Q^2 dependence and $G_A(Q^2)$ reduces to the axial-vector coupling constant in the chiral limit.

For the nucleon-to-delta transition the lowest-order Lagrangian is given by [see Eq. (4.200) of Ref. [48] with $\tilde{z} = -1$]

$$\begin{aligned} \mathcal{L}_{\pi N \Delta}^{(1)} &= \mathbf{g} \sum_{i,j=1}^3 \bar{\Psi}_{\lambda,i} \xi_{ij}^{\frac{3}{2}} (g^{\lambda\mu} - \gamma^\lambda \gamma^\mu) u_{\mu,j} \Psi + \text{H.c.} \\ &\rightarrow \mathbf{g} \sum_{i,j=1}^3 \bar{\Psi}_{\lambda,i} \xi_{ij}^{\frac{3}{2}} (g^{\lambda\mu} - \gamma^\lambda \gamma^\mu) a_{\mu j} \Psi + \text{H.c.}, \end{aligned} \quad (24)$$

where $\Psi_{\lambda,i}$ denotes a vector-spinor isovector-isospinor field. The isovector-isospinor transforms under the $1 \otimes \frac{1}{2} = \frac{3}{2} \oplus \frac{1}{2}$ representation and, thus, contains both isospin 3/2 and isospin 1/2 components. In order to describe the Δ , it is necessary to project onto the isospin-3/2 subspace. The corresponding matrix representation of the projection operator is denoted by $\xi^{\frac{3}{2}}$ and the entries are given by [48]

$$\xi_{ij}^{\frac{3}{2}} = \delta_{ij} - \frac{1}{3}\tau_i\tau_j.$$

Furthermore, in order to identify the coupling to the external axial-vector field $a_{\mu j}$, we made, as in the nucleon case, the replacement $u_{\mu,j} \rightarrow a_{\mu j}$. Considering $j = 3$ and making use of Eq. (4.184) of Ref. [48],

$$\bar{\Psi}_{\lambda,i} \xi_{i3}^{\frac{3}{2}} = \sqrt{\frac{2}{3}} (\bar{\Delta}_\lambda^+ \quad \bar{\Delta}_\lambda^0),$$

we obtain

$$\mathcal{L}_{\text{int}} = \sqrt{\frac{2}{3}} \mathbf{g} (\bar{\Delta}_\lambda^+ \quad \bar{\Delta}_\lambda^0) (g^{\lambda\mu} - \gamma^\lambda \gamma^\mu) a_{\mu 3} \begin{pmatrix} p \\ n \end{pmatrix} + \text{H.c.}$$

Using Eq. (11), the invariant amplitude of $p \rightarrow \Delta^+$ reads

$$\mathcal{M} = i\sqrt{\frac{2}{3}} \mathbf{g} \bar{w}_\lambda(p_f, s_f) g^{\lambda\mu} u(p_i, s_i) \epsilon_{\mu 3}(q).$$

The reduced matrix element [see Eq. (8)] is obtained by multiplying by $\sqrt{3/2}$ and crossing out the factors i and $\epsilon_{\mu 3}(q)$:

$$\bar{w}_\lambda(p_f, s_f) \Gamma_A^{\lambda\mu} u(p_i, s_i) = \mathbf{g} \bar{w}_\lambda(p_f, s_f) g^{\lambda\mu} u(p_i, s_i). \quad (25)$$

A comparison with Eq. (12) then yields the analogue of Eq. (23), namely,

$$C_5^A(Q^2) = \mathbf{g}. \quad (26)$$

Finally, how is this related to the static quark model? For this purpose, we consider

$$\langle \Delta^+(\vec{0}), S_z = 1/2 | A_{z,3}(0) | p(\vec{0}), S_z = 1/2 \rangle = -\sqrt{\frac{2}{3}} \mathbf{g} \bar{w}_3(\vec{0}, S_z = 1/2) u(\vec{0}, S_z = 1/2),$$

where we made use of $g^{33} = -1$. Since $\epsilon_{3,3} = -1$ and $\epsilon_{1,3} + i\epsilon_{2,3} = 0$, we obtain in terms of the appropriate Clebsch-Gordan coefficients,

$$\begin{aligned} w_3(\vec{0}, S_z = 1/2) &= \sqrt{\frac{2}{3}} \epsilon_{3,3} u(\vec{0}, S_z = 1/2) + \frac{1}{\sqrt{3}} \left(-\frac{1}{\sqrt{2}} (\epsilon_{1,3} + i\epsilon_{2,3}) \right) u(\vec{0}, S_z = -1/2) \\ &= -\sqrt{\frac{2}{3}} u(\vec{0}, S_z = 1/2). \end{aligned}$$

Putting the pieces together, the matrix element is given by

$$\begin{aligned} \langle \Delta^+(\vec{0}), S_z = 1/2 | A_{z,3}(0) | p(\vec{0}), S_z = 1/2 \rangle &= -\sqrt{\frac{2}{3}} \mathbf{g} (-1) \sqrt{\frac{2}{3}} \bar{u}(\vec{0}, S_z = 1/2) u(\vec{0}, S_z = 1/2) \\ &= \mathbf{g} \frac{2}{3} \sqrt{2m_\Delta} \sqrt{2m_N}. \end{aligned} \quad (27)$$

Again, when we compare this to Eq. (18) for the static quark model, we have to cross out the normalization factors $\sqrt{2m_\Delta}$ and $\sqrt{2m_N}$. In combination with Eq. (23) we obtain

$$\frac{2}{3} \mathbf{g} = \frac{2}{5} \sqrt{2} \mathbf{g}_A,$$

or

$$\mathbf{g} = \frac{3}{5} \sqrt{2} \mathbf{g}_A. \quad (28)$$

In Table I, we collect the numerical values of the masses and coupling constants which are taken as fixed in the subsequent calculations.

TABLE I. Masses and coupling constants.

Pion mass	$M_\pi = 139.57$ MeV
Nucleon mass	$m_N = 938.92$ MeV
a_1 mass	$M_{a_1} = 1260$ MeV
Pion-decay constant	$F_\pi = 92.2$ MeV
Axial-vector coupling constant	$g_A = 1.2723$
Pion-nucleon coupling constant	$g_{\pi N}^2 / (4\pi) = 13.69$

VI. INCLUSION OF THE a_1 AXIAL-VECTOR MESON

The vector mesons ρ and ω play an important role in the description of the electromagnetic form factors of the nucleon in chiral effective field theory [49–51]. Similarly, the a_1 axial-vector meson leads to an improved description of the axial form factor G_A [35]. Moreover, in the $\gamma^*N \rightarrow \Delta$ transition, the contribution of the ρ meson is needed to obtain a good description of the experimental data [52]. Even though we have rather little experimental data for the axial $N\Delta$ transition [7–11], we expect that the a_1 meson plays a similar role as in the nucleon case. For that reason, we discuss the relevant Lagrangians and calculate their contribution to the form factors.

A. Nucleon

The Lagrangian for the interaction of the a_1 meson with the building block $f_{-\mu\nu}$ is given by [see Eq. (52) of Ref. [53]]

$$-\frac{1}{4}f_A\langle A^{\mu\nu}f_{-\mu\nu}\rangle, \quad (29)$$

where $\langle \dots \rangle$ denotes $\text{Tr}(\dots)$ and

$$\begin{aligned} A^{\mu\nu} &= \nabla^\mu A^\nu - \nabla^\nu A^\mu, \\ \nabla^\mu A^\nu &= \partial^\mu A^\nu + [\Gamma^\mu, A^\nu], \\ \Gamma^\mu &= \frac{1}{2} [u^\dagger(\partial^\mu - ir^\mu)u + u(\partial^\mu - il^\mu)u^\dagger], \\ f_{-\mu\nu} &= uf_{L\mu\nu}u^\dagger - u^\dagger f_{R\mu\nu}u, \\ f_{L\mu\nu} &= \partial_\mu l_\nu - \partial_\nu l_\mu - i[l_\mu, l_\nu], \\ f_{R\mu\nu} &= \partial_\mu r_\nu - \partial_\nu r_\mu - i[r_\mu, r_\nu]. \end{aligned}$$

In comparison with Ref. [53], we omit the roof sign; i.e., we write A^μ instead of \hat{A}^μ . Moreover, we introduce an additional factor $1/\sqrt{2}$, because our normalization of the field matrix is

$$A_\mu = \sum_{i=1}^3 A_{\mu i} \tau_i,$$

whereas Ecker *et al.* use [see Eq. (3.4) of Ref. [54]]

$$A_\mu = \frac{1}{\sqrt{2}} \sum_{i=1}^3 A_{\mu i} \tau_i.$$

The replacement

$$r^\mu \rightarrow a^\mu, \quad l^\mu \rightarrow -a^\mu, \quad f_{-}^{\mu\nu} \rightarrow -2(\partial^\mu a^\nu - \partial^\nu a^\mu),$$

results in the interaction Lagrangian

$$\frac{1}{2}f_A\langle A^{\mu\nu}(\partial_\mu a_\nu - \partial_\nu a_\mu)\rangle = \frac{f_A}{2}(\partial^\mu A_i^\nu - \partial^\nu A_i^\mu)(\partial_\mu a_{\nu i} - \partial_\nu a_{\mu i}).$$

The invariant amplitude for the coupling of an incoming external axial source with four-momentum q , polarization vector ϵ , and isospin component 3 to an outgoing a_1 meson with four-momentum q , polarization vector ϵ_A , and isospin component 3 reads

$$\mathcal{M} = i\frac{f_A}{2}(iq^\mu\epsilon_A^{\nu*} - iq^\nu\epsilon_A^{\mu*})(-iq_\mu\epsilon_\nu + iq_\nu\epsilon_\mu) = if_A\epsilon_{A\nu}^*(q^2g^{\nu\mu} - q^\nu q^\mu)\epsilon_\mu. \quad (30)$$

The lowest-order Lagrangian for the interaction of the a_1 meson with the nucleon is given by [see Eq. (20) of Ref. [35]]

$$\mathcal{L}_{a_1N} = \frac{g_{a_1N}}{2}\bar{\Psi}\gamma^\mu\gamma_5A_\mu\Psi. \quad (31)$$

The corresponding Feynman rule for the absorption of an a_1 meson with isospin index i reads

$$i\frac{g_{a_1N}}{2}\gamma^\mu\gamma_5\tau_i.$$

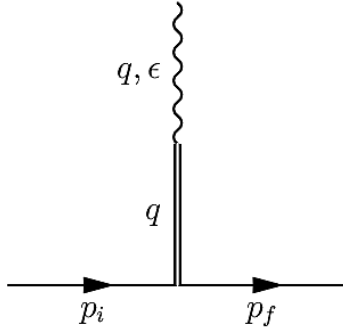


FIG. 1. a_1 contribution to the axial-vector current matrix element between nucleon states.

The contribution to the invariant amplitude for the axial-vector transition induced by $a_{\mu j}(x) = \epsilon_{\mu j}(q)e^{-iq\cdot x}$ is then given by (see Fig. 1)

$$\mathcal{M} = i\frac{g_{a_1N}}{2}\bar{u}(p_f, s_f)\gamma^\rho\gamma_5\tau_j u(p_i, s_i) \left(-g_{\rho\nu} + \frac{q_\rho q_\nu}{M_{a_1}^2}\right) \frac{i}{q^2 - M_{a_1}^2} if_A(q^2g^{\nu\mu} - q^\nu q^\mu)\epsilon_{\mu j}(q).$$

Note that

$$q_\nu(q^2g^{\nu\mu} - q^\nu q^\mu) = q^\mu q^2 - q^2 q^\mu = 0.$$

We thus obtain

$$\mathcal{M} = i\frac{f_A g_{a_1N}}{2} \frac{1}{q^2 - M_{a_1}^2} [q^2\bar{u}(p_f, s_f)\gamma^\mu\gamma_5\tau_j u(p_i, s_i) - q^\mu\bar{u}(p_f, s_f)\not{q}\gamma_5\tau_j u(p_i, s_i)] \epsilon_{\mu j}(q).$$

Making use of $\bar{u}(p_f, s_f)\not{q}\gamma_5 u(p_i, s_i) = 2m_N\bar{u}(p_f, s_f)\gamma_5 u(p_i, s_i)$, we can then read off the contributions to G_A and G_P :⁴

$$G_A : f_A g_{a_1N} \frac{Q^2}{M_{a_1}^2 + Q^2}, \quad (32)$$

$$G_P : f_A g_{a_1N} \frac{4m_N^2}{M_{a_1}^2 + Q^2}. \quad (33)$$

⁴ Note that, due to a typo, Eqs. (46) and (47) of Ref. [35] contain an overall opposite sign.

In essence, the loop diagrams play no role in the one-loop calculation of the axial form factor G_A . In terms of the low-energy constants (LECs) of the Lagrangian of Ref. [55], one obtains

$$G_A(Q^2) = \mathbf{g}_A + 4d_{16}M_\pi^2 - d_{22}Q^2, \quad (34)$$

where d_{16} provides a quark-mass correction to the axial-vector coupling constant, $g_A = \mathbf{g}_A + 4d_{16}M_\pi^2$, and d_{22} is related to the mean-square axial radius. In other words, the low- Q^2 behavior is encoded in two constants g_A and $\langle r_A^2 \rangle$ which chiral symmetry does not predict:

$$G_A^{\text{linear}}(Q^2) = g_A \left(1 - \frac{1}{6} \langle r_A^2 \rangle Q^2 \right). \quad (35)$$

Experimental data are commonly analyzed in terms of the dipole parametrization,

$$G_A^{\text{dipole}}(Q^2) = \frac{g_A}{\left(1 + \frac{Q^2}{M_A^2} \right)^2}, \quad (36)$$

where the parameter M_A is referred to as the axial mass. The weighted average extracted from (quasi)elastic neutrino and antineutrino scattering experiments is $M_A = (1.026 \pm 0.021)$ GeV [3] corresponding to a mean-square axial radius $\langle r_A^2 \rangle = (0.444 \pm 0.018)$ fm². A subsequent re-analysis of quasielastic data on deuterium has reported $M_A = (1.016 \pm 0.026)$ GeV [$\langle r_A^2 \rangle = (0.453 \pm 0.023)$ fm²] [56]. Table II shows the results for M_A reported by more recent experiments on neutrino-nucleus cross sections. The extraction of the single-nucleon form factors from data on nuclei is a challenging endeavor. Therefore, these numbers have to be treated with some caution, because they heavily rely on the theoretical input/model used in the extraction. In particular, some important ingredients were previously missing such as the n particle n hole excitation mechanism proposed in Ref. [62]. Moreover, in contrast to electron-scattering experiments, the extraction is made more complex by the fact that one has to deal with a spectrum of incident neutrinos rather than a monochromatic neutrino beam. For a detailed review on both the experimental and theoretical sides of this topic, see Ref. [63]. For a discussion of theoretical studies abandoning the dipole form in their analyses, see, e.g., Refs. [64–68]. The weighted average extracted from charged pion electroproduction experiments is $M_A = (1.069 \pm 0.016)$ GeV [3] resulting in $\langle r_A^2 \rangle = (0.409 \pm 0.012)$ fm².

TABLE II. Axial masses reported by recent (quasi)elastic neutrino and antineutrino scattering experiments.

Experiment	M_A [GeV]
K2K [57]	1.20 ± 0.12
NOMAD [58]	1.05 ± 0.06
MiniBooNE [59]	1.35 ± 0.17
MINERvA [60]	0.99
MINOS [61]	$1.23_{-0.09}^{+0.13}(\text{fit})_{-0.15}^{+0.12}(\text{syst})$

Including the a_1 meson, the axial form factor may be written as

$$G_A(Q^2) = g_A + c_1 Q^2 + c_2 \frac{Q^2}{M_{a_1}^2 + Q^2} \quad (37)$$

$$= g_A \left[1 + \tilde{c}_1 Q^2 - \tilde{c}_2 \frac{(Q^2)^2}{M_{a_1}^2 (M_{a_1}^2 + Q^2)} \right], \quad (38)$$

where $g_A \tilde{c}_1 = c_1 + c_2/M_{a_1}^2$ and $g_A \tilde{c}_2 = c_2 = f_A g_{a_1 N}$. The structure of the first two terms on the right-hand side of Eq. (37) is the same as that of Eq. (34) but one has to keep in mind that the LEC d_{22} will have a different value in the theory including the a_1 meson. Introducing the normalized axial form factor as

$$F_A(Q^2) = \frac{G_A(Q^2)}{G_A(0)}, \quad (39)$$

the parametrization of $F_A(Q^2)$ contains two parameters, namely, \tilde{c}_1 and \tilde{c}_2 , which can be determined from a fit to experimental data. Expanding the normalized axial form factor as

$$F_A(Q^2) = 1 - \frac{1}{6} \langle r_A^2 \rangle Q^2 + \frac{1}{120} \langle r_A^4 \rangle (Q^2)^2 + \dots, \quad (40)$$

for the parametrization including the a_1 meson, Eq. (38), we can identify the mean-square and mean-quartic axial radii as

$$\langle r_A^2 \rangle = -6\tilde{c}_1, \quad \langle r_A^4 \rangle = -120 \frac{\tilde{c}_2}{M_{a_1}^4}, \quad (41)$$

respectively. On the other hand, for the dipole parametrization, Eq. (36), one obtains

$$\langle r_A^2 \rangle = \frac{12}{M_A^2}, \quad \langle r_A^4 \rangle = \frac{360}{M_A^4}. \quad (42)$$

Figure 2 shows the results of fitting the dipole parametrization to experimental data extracted from pion electroproduction experiments [3].⁵ The fits are performed for different values of the maximal squared momentum transfer, Q_{\max}^2 , and the corresponding axial masses, mean-square axial radii, and mean-quartic axial radii are summarized in Table III.⁶ In their common domain, the curves associated with $Q_{\max}^2 = 0.6 \text{ GeV}^2$ and $Q_{\max}^2 = 1 \text{ GeV}^2$ are hardly distinguishable in Fig. 2, because the difference between the fitted axial masses is very small.

Figure 3 shows the corresponding fits using the parametrization of Eq. (38) including the a_1 meson (a_1 fits for short). The respective parameters \tilde{c}_1 and \tilde{c}_2 , mean-square axial radii, and mean-quartic axial radii are summarized in Table IV. When comparing the a_1 fit to the dipole fit, one should keep in mind that Eq. (38) represents a model for the low- Q^2 behavior

⁵ We would like to thank U.-G. Meißner for providing the data in the form of a table.

⁶ Strictly speaking, because of a loop correction to the threshold electric dipole amplitude E_{0+} , the mean-square axial radius extracted from pion electroproduction has to be modified by an amount

$$\frac{3}{64F_\pi^2} \left(\frac{12}{\pi^2} - 1 \right) = 0.0456 \text{ fm}^2,$$

such that the true axial radius is slightly larger [3, 69]. This is consistent with the observation that the average for M_A extracted from charged pion electroproduction experiments is larger than the value from (quasi)elastic neutrino and antineutrino scattering experiments.

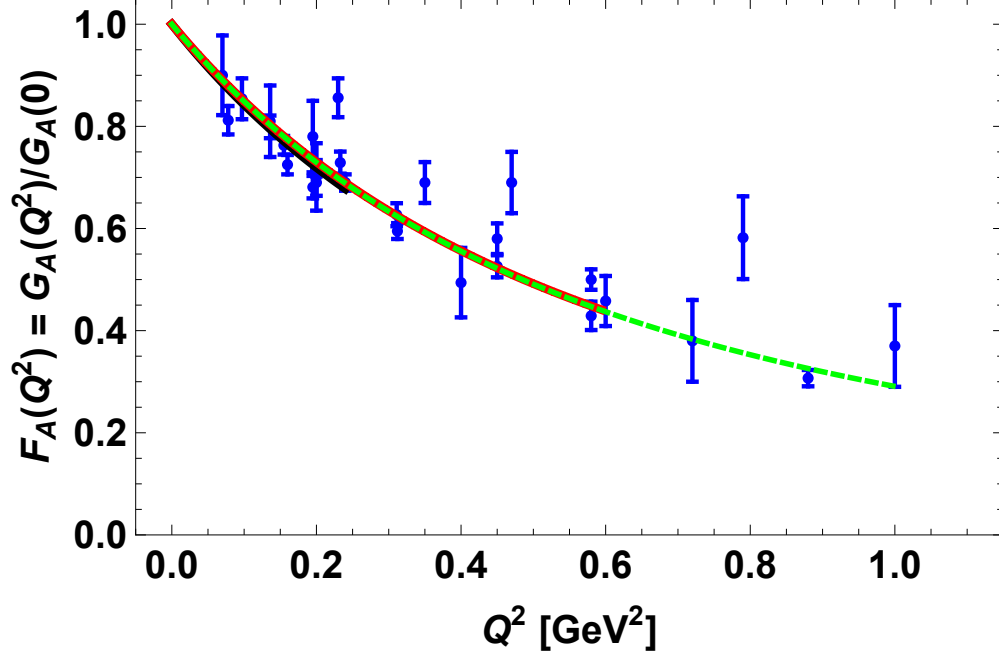


FIG. 2. (Color online) $F_A(Q^2) = G_A(Q^2)/G_A(0)$ fitted to different ranges of momentum transfer Q^2 using the dipole parametrization of Eq. (36). The (black) solid line corresponds to a fit up to and including $Q_{\max}^2 = 0.24$ GeV^2 , the (red) long-dashed line up to and including $Q_{\max}^2 = 0.6$ GeV^2 , and the (green) short-dashed line up to and including $Q_{\max}^2 = 1$ GeV^2 , respectively. The corresponding parameters are given in Table III.

TABLE III. Comparison of the axial masses, mean-square axial radii, and mean-quartic axial radii obtained from the dipole expression of the form factor F_A fitted to different ranges of momentum transfer.

Q_{\max}^2 [GeV^2]	M_A [GeV]	$\langle r_A^2 \rangle$ [fm^2]	$\langle r_A^4 \rangle$ [fm^4]	χ_{red}^2
0.24	1.057 ± 0.027	0.418 ± 0.021	0.437 ± 0.045	2.87
0.6	1.084 ± 0.020	0.398 ± 0.015	0.395 ± 0.029	3.21
1.0	1.082 ± 0.019	0.399 ± 0.014	0.398 ± 0.028	2.97

of the axial form factor with a restricted domain of validity. The fits of Fig. 3 share the common feature that F_A , when extrapolated beyond Q_{\max}^2 , very soon starts to rise again and diverges as $Q^2 \rightarrow \infty$. This is, of course, an unphysical feature, originating from the linear term proportional to c_1 in Eq. (37). Moreover, the a_1 contribution asymptotically does not fall off as $1/(Q^2)^2$ as predicted by perturbative QCD [70].⁷ Motivated by the observation that the dipole fit and the a_1 fit produce similar results for $Q_{\max}^2 = 0.6$ GeV^2 , we will, somewhat arbitrarily, assume that this value provides a reasonable upper limit for the range of applicability of the a_1 model. According to Eqs. (37) and (41), the mean-square axial

⁷ Note that the dipole form shows this behavior.

radius obtains a contribution from both the low-energy constant (LEC) c_1 and the a_1 -pole diagram (see Fig. 1). For the values of \tilde{c}_1 and \tilde{c}_2 of Table IV, the a_1 contribution to $\langle r_A^2 \rangle$ is larger than the total result, implying a negative contribution from the LEC c_1 . To be specific, for $Q_{\max}^2 = 0.6 \text{ GeV}^2$ we obtain $\langle r_A^2 \rangle_{\text{LEC}} + \langle r_A^2 \rangle_{a_1} = (-0.366 + 0.781) \text{ fm}^2 = 0.415 \text{ fm}^2$.

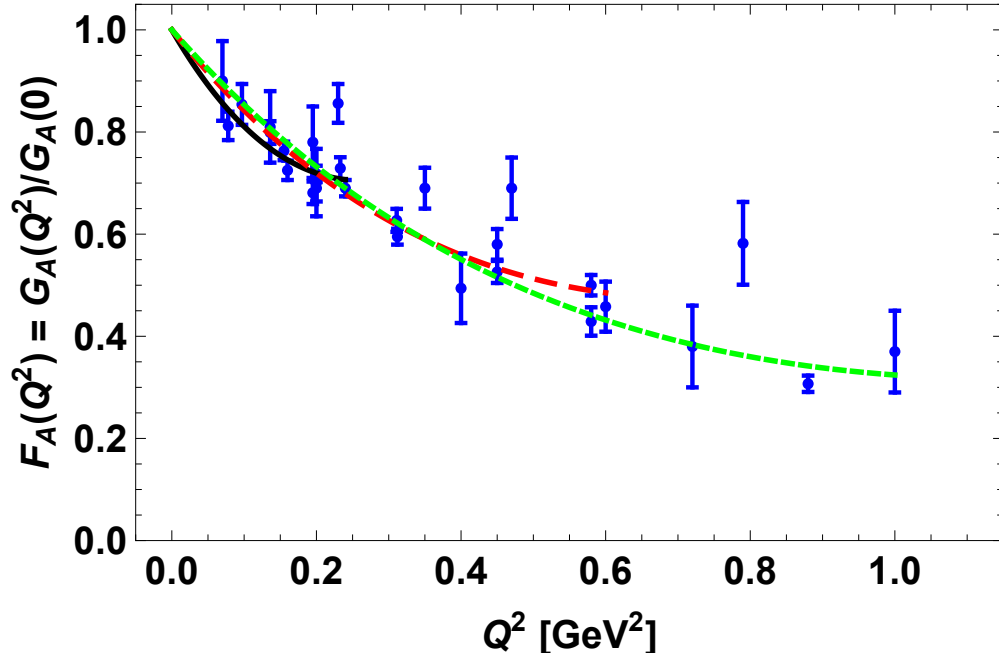


FIG. 3. (Color online) $F_A(Q^2) = G_A(Q^2)/G_A(0)$ fitted to different ranges of momentum transfer Q^2 using the parametrization of Eq. (38) including the a_1 meson. The (black) solid line corresponds to a fit up to and including $Q_{\max}^2 = 0.24 \text{ GeV}^2$, the long-dashed (red) line up to and including $Q_{\max}^2 = 0.6 \text{ GeV}^2$, and the short-dashed (green) line up to and including $Q_{\max}^2 = 1 \text{ GeV}^2$, respectively. The corresponding parameters are given in Table IV.

TABLE IV. Comparison of the parameters \tilde{c}_1 and \tilde{c}_2 , mean-square axial radii, and mean-quartic axial radii obtained from the expression Eq. (37) of the form factor F_A fitted to different ranges of momentum transfer.

Q_{\max}^2 [GeV ²]	\tilde{c}_1 [GeV ⁻²]	\tilde{c}_2	$\langle r_A^2 \rangle$ [fm ²]	$\langle r_A^4 \rangle$ [fm ⁴]	χ_{red}^2
0.24	-2.44 ± 0.32	-14.8 ± 4.4	0.570 ± 0.075	1.068 ± 0.318	2.08
0.6	-1.78 ± 0.09	-5.31 ± 0.69	0.416 ± 0.021	0.383 ± 0.050	2.68
1.0	-1.61 ± 0.07	-3.84 ± 0.39	0.376 ± 0.016	0.277 ± 0.028	3.27

At order $\mathcal{O}(p^3)$ in chiral perturbation theory, the low- Q^2 behavior of the induced pseudoscalar form factor $G_P(Q^2)$ can entirely be written in terms of known physical quantities [35, 40],

$$G_P(Q^2) = 4 \frac{m_N F_\pi g_{\pi N}}{M_\pi^2 + Q^2} - \frac{2}{3} m_N^2 g_A \langle r_A^2 \rangle, \quad (43)$$

where $g_{\pi N}$ denotes the pion-nucleon coupling constant with $g_{\pi N}^2/(4\pi) = 13.69 \pm 0.19$ [71]. Using Eq. (33), the relevant expression including the a_1 meson reads

$$G_P(Q^2) = 4 \frac{m_N F_\pi g_{\pi N}}{M_\pi^2 + Q^2} - \frac{2}{3} m_N^2 g_A \langle r_A^2 \rangle - 4m_N^2 g_A \tilde{c}_2 \frac{Q^2}{M_{a_1}^2 (M_{a_1}^2 + Q^2)}, \quad (44)$$

where the mean-square axial radius is given in Eq. (41). In Fig. 4, we compare the results for $G_P(Q^2)$ including the a_1 contribution (solid line) and without the a_1 contribution (dashed line). Clearly, at low Q^2 , the form factor is dominated by the pion-pole contribution and a deviation due to the a_1 meson is only seen for larger values of Q^2 , where the form factor is small.

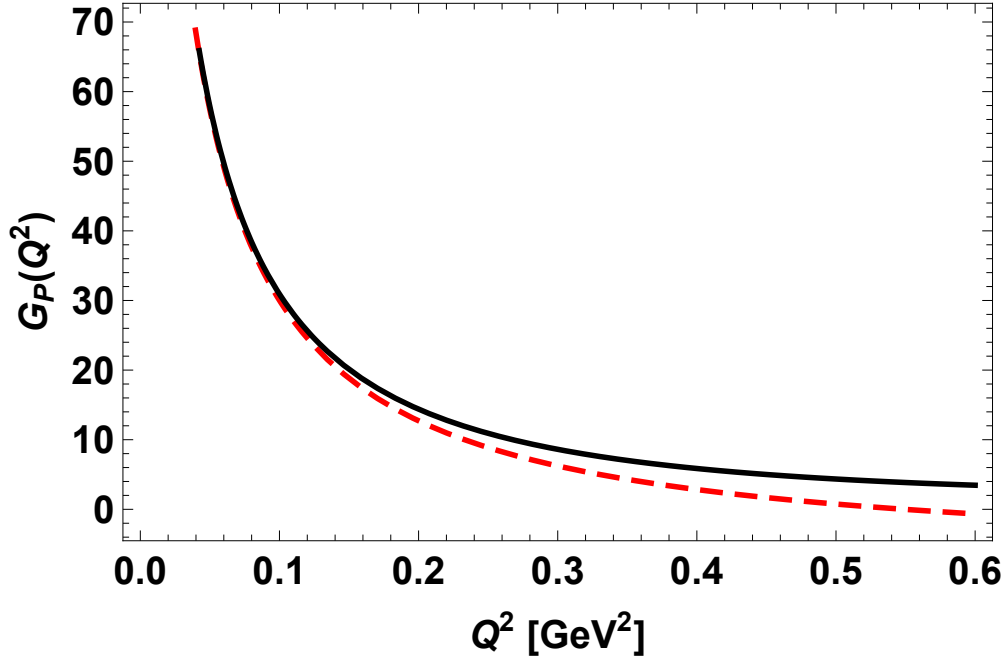


FIG. 4. (Color online) Induced pseudoscalar form factor $G_P(Q^2)$. (Red) dashed line: Pion-pole dominance result. (Black) solid line: Result including the a_1 meson.

B. Nucleon-to-delta transition

In order to discuss the a_1 -meson contribution to $C_5^A(Q^2)$ and $C_6^A(Q^2)$, we need the coupling of the a_1 meson to the $N\Delta$ system. We model this interaction in analogy to the coupling of the external axial-vector field $a_{\mu j}(x)$ [see Eqs. (22) and (24)]. For the neutral a_1 meson we obtain

$$\mathcal{L}_{a_1 N \Delta} = g_{a_1 N \Delta} \sqrt{\frac{2}{3}} (\bar{\Delta}_\lambda^+ \quad \bar{\Delta}_\lambda^0) (g^{\lambda\mu} - \gamma^\lambda \gamma^\mu) A_{\mu 3} \begin{pmatrix} p \\ n \end{pmatrix} + \text{H.c.} \quad (45)$$

In particular, since the external axial-vector field $a_{\mu j}(x)$ and the field $A_{\mu j}(x)$ carry the same quantum numbers, it is natural to assume the same SU(6) relation for the coupling constants

$g_{a_1 N}$ and $g_{a_1 N \Delta}$ as for \mathbf{g}_A and \mathbf{g} [see Eq. (28)],

$$g_{a_1 N \Delta} = \frac{3}{5} \sqrt{2} g_{a_1 N}. \quad (46)$$

The contribution of the a_1 meson to $C_5^A(Q^2)$ is obtained from Eq. (26) by the replacement

$$\mathbf{g} \rightarrow f_A g_{a_1 N \Delta} \frac{Q^2}{M_{a_1}^2 + Q^2}.$$

As in the nucleon case, the loop contributions to the low- Q^2 behavior of $C_5^A(Q^2)$ are small [72] and we can write

$$C_5^A(Q^2) = g_{AN\Delta} + c_3 Q^2 + c_4 \frac{Q^2}{M_{a_1}^2 + Q^2}, \quad (47)$$

where $c_4 = f_A g_{a_1 N \Delta}$. Extracting $C_5^A(0) = g_{AN\Delta}$, we get

$$C_5^A(Q^2) = g_{AN\Delta} \left[1 + \tilde{c}_3 Q^2 - \tilde{c}_4 \frac{(Q^2)^2}{M_{a_1}^2 (M_{a_1}^2 + Q^2)} \right], \quad (48)$$

where $g_{AN\Delta} \tilde{c}_3 = c_3 + c_4/M_{a_1}^2$ and $\tilde{c}_4 = c_4/g_{AN\Delta}$. By analogy with Eq. (41), we find for the mean-square and mean-quartic axial transition radii

$$\langle r_{AN\Delta}^2 \rangle = -6\tilde{c}_3, \quad \langle r_{AN\Delta}^4 \rangle = -120 \frac{\tilde{c}_4}{M_{a_1}^2}. \quad (49)$$

At this point, we make use of the quark-model relation of Eq. (46) between the coupling constants $g_{a_1 N \Delta}$ and $g_{a_1 N}$ to reexpress \tilde{c}_4 as

$$\tilde{c}_4 = \frac{f_A g_{a_1 N \Delta}}{g_{AN\Delta}} = \frac{3}{5} \sqrt{2} \frac{f_A g_{a_1 N}}{g_{AN\Delta}} = \frac{3}{5} \sqrt{2} \frac{g_A}{g_{AN\Delta}} \tilde{c}_2.$$

Applying, in addition, to $g_{AN\Delta}$ and g_A the quark-model relation of Eq. (28), we obtain the simple result

$$\tilde{c}_4 = \tilde{c}_2. \quad (50)$$

With these assumptions, the form factor $C_5^A(Q^2)$ contains only one single free parameter \tilde{c}_3 (or c_3). In order to show the dependence on this parameter, as a starting point we make use of the assumption

$$C_5^A(Q^2) = g_{AN\Delta} F_A(Q^2) = \frac{3}{5} \sqrt{2} G_A(Q^2), \quad (51)$$

i.e., $\tilde{c}_3 = \tilde{c}_1$, and then vary the LEC \tilde{c}_3 . Figure 5 shows a comparison between $G_A(Q^2)$ and $C_5^A(Q^2)$. The parameters for $G_A(Q^2)$ [(black) long-dashed line] are taken from the fit with $Q_{\max}^2 = 0.6 \text{ GeV}^2$ (second row of Table IV). The (black) solid line corresponds to Eq. (51) for $C_5^A(Q^2)$, the (blue) short-dashed line and the (red) dashed line correspond to a decrease and an increase of the mean-square axial transition radius by 5 %, respectively.

By analogy with Eq. (43), the low- Q^2 behavior of $C_6^A(Q^2)$ without the a_1 meson can be written as (see Appendix B)

$$C_6^A(Q^2) = \frac{m_N F_\pi g_{\pi N \Delta}}{M_\pi^2 + Q^2} + m_N^2 C_5^{A'}(0), \quad (52)$$

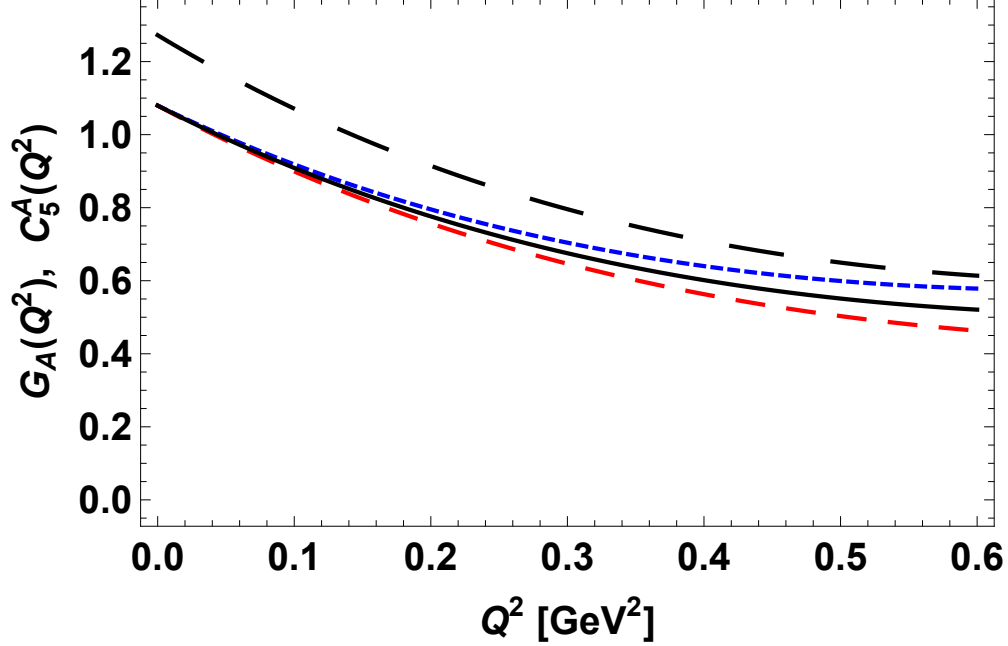


FIG. 5. (Color online) Axial form factor of the nucleon $G_A(Q^2)$ [(black) long-dashed line]. Axial $N\Delta$ transition form factor $C_5^A(Q^2)$: The (black) solid line corresponds to Eq. (51), the (blue) short-dashed and (red) dashed lines correspond to a decrease and an increase of the mean-square axial transition radius by 5%, respectively.

where $g_{\pi N\Delta} = G_{\pi N\Delta}(-M_\pi^2)$ is the pion-nucleon- Δ coupling constant. Including the a_1 meson, we obtain

$$C_6^A(Q^2) = \frac{m_N F_\pi g_{\pi N\Delta}}{M_\pi^2 + Q^2} + m_N^2 C_5^{A'}(0) - m_N^2 g_{AN\Delta} \tilde{c}_4 \frac{Q^2}{M_{a_1}^2 (M_{a_1}^2 + Q^2)}. \quad (53)$$

In terms of the lowest-order Lagrangian, Eq. (24), and the lowest-order prediction $g_{AN\Delta} = \mathbf{g}$, Eq. (26), the pion-nucleon- Δ coupling constant satisfies the generalization of the Goldberger-Treiman relation [73, 74],⁸

$$g_{\pi N\Delta} = \frac{m_N}{F_\pi} g_{AN\Delta}. \quad (54)$$

Using $\tilde{c}_2 = \tilde{c}_4$ of Eq. (50) and the quark-model relation $g_{AN\Delta} = 3\sqrt{2}g_A/5$, we obtain the following prediction,

$$\begin{aligned} C_6^A(Q^2) &= \frac{3\sqrt{2}}{20} G_P(Q^2) + m_N^2 \left(C_5^{A'}(0) - \frac{3}{5} \sqrt{2} G_A'(0) \right) \\ &= \frac{3\sqrt{2}}{20} G_P(Q^2) - \frac{1}{6} m_N^2 \left(\langle r_{AN\Delta}^2 \rangle - \frac{3}{5} \sqrt{2} \langle r_A^2 \rangle \right), \end{aligned} \quad (55)$$

where $G_P(Q^2)$ is the induced pseudoscalar form factor of Eq. (44). At this stage, we assume that $G_A'(0) = c_1$ and $C_5^{A'}(0) = c_3$ are independent. Figure 6 shows a comparison between

⁸ Using the values of Table I, the Goldberger-Treiman discrepancy at the nucleon level, $\Delta = 1 - m_N g_A / (F_\pi g_{\pi N})$, amounts to $\Delta = 1.2\%$.

$C_6^A(Q^2)$ without and including the a_1 meson. In each case we make use of the quark-model estimate $g_{\pi N\Delta} = 3\sqrt{2}g_{\pi N}/5$ as obtained from the respective Goldberger-Treiman relations. The (black) long-dashed line corresponds to Eq. (52) with $C_5^{A'}(0) = g_{AN\Delta}\tilde{c}_1$ and $\tilde{c}_1 = -1.78 \text{ GeV}^{-2}$. For the result that includes the a_1 we assume, in addition, $\tilde{c}_4 = \tilde{c}_2 = -5.31$ (second row of Table IV). The (black) solid line corresponds to Eq. (53) for $C_6^A(Q^2)$, the (blue) short-dashed line and the (red) dashed line correspond to a decrease and an increase of the mean-square axial transition radius by 10 %, respectively.

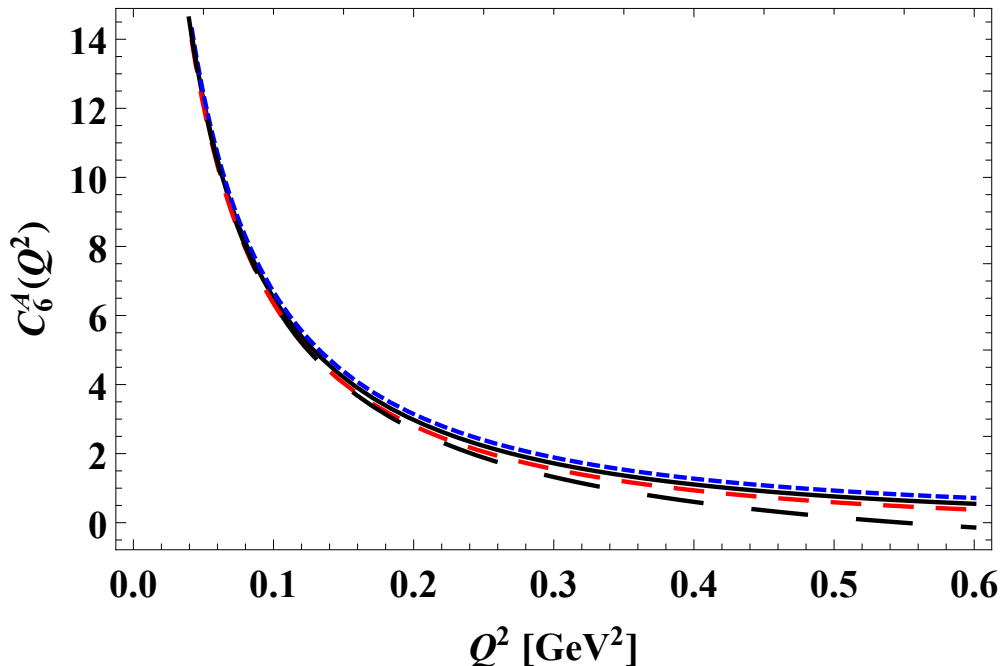


FIG. 6. (Color online) Axial nucleon-to-nucleon transition form factor $C_6^A(Q^2)$. (Black) long-dashed line: Pion-pole-dominance result of Eq. (52). The (black) solid line corresponds to Eq. (55), the (blue) short-dashed and (red) dashed lines correspond to a decrease and an increase of the mean-square axial transition radius by 10%, respectively.

VII. SUMMARY AND CONCLUSIONS

We analyzed the low- Q^2 behavior of the axial form factor $G_A(Q^2)$, the induced pseudoscalar form factor $G_P(Q^2)$, and the axial nucleon-to-delta transition form factors $C_5^A(Q^2)$ and $C_6^A(Q^2)$. To this end we made use of a chiral effective Lagrangian for the interaction of the a_1 meson with an external axial current, the nucleon, and the Δ . Within this approach, the axial form factor $G_A(Q^2)$ is described in terms of three parameters [see Eq. (37)]. We investigated the parameters by fitting the model to empirical data, choosing different values of the maximal squared momentum transfer (see Table IV). We compared the results with the commonly used dipole parametrization (see Figs. 2 and 3). Extending a relation known from chiral perturbation theory, we made a prediction for the induced pseudoscalar form factor $G_P(Q^2)$. For the determination of the transition form factor $C_5^A(Q^2)$ we drew on an SU(6) spin-flavor quark-model relation to fix $g_{AN\Delta}$ and $g_{a_1N\Delta}$ in terms of g_A and g_{a_1N} ,

respectively. With this assumption, the result for $C_5^A(Q^2)$ depends only on a single parameter \tilde{c}_3 , which is related to the mean-square axial transition radius (see Fig. 5). Finally, the transition form factor $C_6^A(Q^2)$ was predicted in terms of $G_P(Q^2)$, and the derivatives $G_A'(0)$ and $C_5^{A'}(0)$. We emphasize that the predictions at hand represent a model of the relevant form factors at low Q^2 . To be specific, we expect $Q^2 = 0.6 \text{ GeV}^2$ to be a reasonable upper limit for the applicability of the model.

The purpose of the present investigation was to identify the a_1 meson as an important messenger particle in the context of axial-vector current transitions. The use of SU(6) spin-flavor quark-model relations has to be regarded as a first attempt to restrict the number of free parameters. Clearly, merging the a_1 -meson contribution with the inclusion of pion loops within a consistent power counting is a desirable next step. However, as far as the predictive power is concerned, one has to keep in mind that the chiral effective field theory calculation will essentially contain the same number of free parameters, i.e., LECs.

ACKNOWLEDGMENTS

Y. Ü. and A. K. would like to thank the Collaborative Research Center 1044 of the German Research Foundation for financial support during their stay in Mainz. The work of Y. Ü. was supported by the Scientific and Technological Research Council of Turkey (TÜBİTAK).

Appendix A: Conventions for Dirac spinors

For the normalization of spinors and states, we follow Appendix A of Ref. [47]. We only include the relations which are necessary for our calculation.

$$\begin{aligned}
\langle \vec{p}', r | \vec{p}, s \rangle &= 2E(\vec{p})(2\pi)^3 \delta^3(\vec{p}' - \vec{p}) \delta_{rs}, \\
E(\vec{p}) &= \sqrt{m^2 + \vec{p}^2}, \\
|N(\vec{p}, s)\rangle &= b_s^\dagger(\vec{p})|0\rangle, \\
\{b_r(\vec{p}'), b_s^\dagger(\vec{p})\} &= 2E(\vec{p})(2\pi)^3 \delta^3(\vec{p}' - \vec{p}) \delta_{rs}, \\
\Psi(x) &= \sum_{r=1}^2 \int \frac{d^3p}{2E(\vec{p})(2\pi)^3} (b_r(\vec{p})u^{(r)}(\vec{p})e^{-ip \cdot x} + d_r^\dagger(\vec{p})v^{(r)}(\vec{p})e^{ip \cdot x}), \\
p^0 &= E(\vec{p}), \\
u^{(r)}(\vec{p}) &= \sqrt{E(\vec{p}) + m} \begin{pmatrix} \chi_r \\ \frac{\vec{\sigma} \cdot \vec{p}}{E(\vec{p}) + m} \chi_r \end{pmatrix}, \\
\chi_1 &= \begin{pmatrix} 1 \\ 0 \end{pmatrix}, \quad \chi_2 = \begin{pmatrix} 0 \\ 1 \end{pmatrix}, \\
\bar{u}^{(r)}(\vec{p})u^{(s)}(\vec{p}) &= 2m\delta_{rs}, \\
\langle 0 | \Psi(x) | N(\vec{p}, s) \rangle &= u^{(s)}(\vec{p})e^{-ip \cdot x}.
\end{aligned}$$

Appendix B: Low- Q^2 expansion of $C_6^A(Q^2)$

We define the pion-nucleon- Δ form factor $G_{\pi N\Delta}(Q^2)$ in terms of the reduced matrix element

$$\langle \Delta(p_f, s_f) | \hat{m} P^{(1)} | N(p_i, s_i) \rangle = \frac{M_\pi^2 F_\pi}{M_\pi^2 + Q^2} G_{\pi N\Delta}(Q^2) i \bar{w}_\lambda(p_f, s_f) \frac{q^\lambda}{m_N} u(p_i, s_i). \quad (\text{B1})$$

Using the parametrization of Eq. (12), the equation for the divergence of the axial-vector current, Eq. (2), results in

$$C_5^A(Q^2) - \frac{Q^2}{m_N^2} C_6^A(Q^2) = \frac{M_\pi^2 F_\pi}{M_\pi^2 + Q^2} \frac{G_{\pi N\Delta}(Q^2)}{m_N}. \quad (\text{B2})$$

Truncating the expansion of the form factors $C_5^A(Q^2)$ and $G_{\pi N\Delta}(Q^2)$ after the linear order in Q^2 ,

$$\begin{aligned} C_5^A(Q^2) &= C_5^A(0) + Q^2 C_5^{A'}(0), \\ G_{\pi N\Delta}(Q^2) &= G_{\pi N\Delta}(0) + Q^2 G_{\pi N\Delta}'(0), \end{aligned}$$

and using

$$g_{\pi N\Delta} = G_{\pi N\Delta}(-M_\pi^2) = G_{\pi N\Delta}(0) - M_\pi^2 G_{\pi N\Delta}'(0),$$

we obtain

$$\begin{aligned} C_6^A(Q^2) &= \frac{m_N^2}{Q^2} \left[C_5^A(Q^2) - \frac{M_\pi^2 F_\pi}{M_\pi^2 + Q^2} \frac{G_{\pi N\Delta}(Q^2)}{m_N} \right] \\ &= \frac{m_N^2}{Q^2} \frac{1}{M_\pi^2 + Q^2} \left[(M_\pi^2 + Q^2)(C_5^A(0) + Q^2 C_5^{A'}(0)) - \frac{M_\pi^2 F_\pi}{m_N} (G_{\pi N\Delta}(0) + Q^2 G_{\pi N\Delta}'(0)) \right] \\ &= \frac{m_N^2}{Q^2(Q^2 + M_\pi^2)} \left[M_\pi^2 C_5^A(0) + M_\pi^2 Q^2 C_5^{A'}(0) + Q^2 C_5^A(0) + (Q^2)^2 C_5^{A'}(0) \right. \\ &\quad \left. - \frac{M_\pi^2 F_\pi}{m_N} G_{\pi N\Delta}(0) - \frac{M_\pi^2 F_\pi}{m_N} Q^2 G_{\pi N\Delta}'(0) \right] \\ &= \frac{m_N^2}{M_\pi^2 + Q^2} \left[C_5^A(0) - M_\pi^2 \frac{F_\pi}{m_N} G_{\pi N\Delta}'(0) + (M_\pi^2 + Q^2) C_5^{A'}(0) \right] \\ &= \frac{m_N^2}{M_\pi^2 + Q^2} \left[\frac{F_\pi G_{\pi N\Delta}(0)}{m_N} - M_\pi^2 \frac{F_\pi}{m_N} G_{\pi N\Delta}'(0) + (M_\pi^2 + Q^2) C_5^{A'}(0) \right] \\ &= \frac{m_N F_\pi g_{\pi N\Delta}}{M_\pi^2 + Q^2} + m_N^2 C_5^{A'}(0). \end{aligned}$$

-
- [1] C. F. Perdrisat, V. Punjabi, and M. Vanderhaeghen, Prog. Part. Nucl. Phys. **59**, 694 (2007).
 - [2] S. Pacetti, R. Baldini Ferroli, and E. Tomasi-Gustafsson, Phys. Rept. **550-551**, 1 (2015).
 - [3] V. Bernard, L. Elouadrhiri, and U.-G. Meißner, J. Phys. G **28**, R1 (2002).
 - [4] T. Gorringer and H. W. Fearing, Rev. Mod. Phys. **76**, 31 (2004).

- [5] L. Tiator, D. Drechsel, S. S. Kamalov, and M. Vanderhaeghen, *Eur. Phys. J. ST* **198**, 141 (2011).
- [6] I. G. Aznauryan and V. D. Burkert, *Prog. Part. Nucl. Phys.* **67**, 1 (2012).
- [7] S. J. Barish *et al.*, *Phys. Rev. D* **19**, 2521 (1979).
- [8] G. M. Radecky *et al.*, *Phys. Rev. D* **25**, 1161 (1982) Erratum: [*Phys. Rev. D* **26**, 3297 (1982)].
- [9] T. Kitagaki *et al.*, *Phys. Rev. D* **34**, 2554 (1986).
- [10] T. Kitagaki *et al.*, *Phys. Rev. D* **42**, 1331 (1990).
- [11] D. Androic *et al.* [G0 Collaboration], arXiv:1212.1637 [nucl-ex] (2012).
- [12] J. G. Körner, T. Kobayashi, and C. Avilez, *Phys. Rev. D* **18**, 3178 (1978).
- [13] T. R. Hemmert, B. R. Holstein, and N. C. Mukhopadhyay, *Phys. Rev. D* **51**, 158 (1995).
- [14] J. Lú, N. C. Mukhopadhyay, and L. Zhang, *Phys. Rev. C* **52**, 1630 (1995).
- [15] B. Golli, S. Sirca, L. Amoreira, and M. Fiolhais, *Phys. Lett. B* **553**, 51 (2003).
- [16] D. Barquilla-Cano, A. J. Buchmann, and E. Hernandez, *Phys. Rev. C* **75**, 065203 (2007) Erratum: [*Phys. Rev. C* **77**, 019903 (2008)].
- [17] S. L. Zhu and M. J. Ramsey-Musolf, *Phys. Rev. D* **66**, 076008 (2002).
- [18] L. S. Geng, J. Martin Camalich, L. Alvarez-Ruso, and M. J. Vicente Vacas, *Phys. Rev. D* **78**, 014011 (2008).
- [19] M. Procura, *Phys. Rev. D* **78**, 094021 (2008).
- [20] C. Alexandrou, T. Leontiou, J. W. Negele, and A. Tsapalis, *Phys. Rev. Lett.* **98**, 052003 (2007).
- [21] C. Alexandrou, G. Koutsou, T. Leontiou, J. W. Negele, and A. Tsapalis, *Phys. Rev. D* **76**, 094511 (2007) Erratum: [*Phys. Rev. D* **80**, 099901 (2009)].
- [22] C. Alexandrou, E. B. Gregory, T. Korzec, G. Koutsou, J. W. Negele, T. Sato, and A. Tsapalis, *Phys. Rev. D* **87**, 114513 (2013).
- [23] T. M. Aliev, K. Azizi, and A. Ozpineci, *Nucl. Phys. A* **799**, 105 (2008).
- [24] A. Küçükarslan, U. Ozdem, and A. Ozpineci, *Nucl. Phys. B* **913**, 132 (2016).
- [25] S. L. Adler, *Annals Phys.* **50**, 189 (1968).
- [26] C. H. Llewellyn Smith, *Phys. Rept.* **3**, 261 (1972).
- [27] P. A. Schreiner and F. Von Hippel, *Nucl. Phys. B* **58**, 333 (1973).
- [28] S. L. Adler, *Phys. Rev. D* **12**, 2644 (1975).
- [29] N. C. Mukhopadhyay, M. J. Ramsey-Musolf, S. J. Pollock, J. Liu, and H. W. Hammer, *Nucl. Phys. A* **633**, 481 (1998).
- [30] L. Alvarez-Ruso, S. K. Singh, and M. J. Vicente Vacas, *Phys. Rev. C* **59**, 3386 (1999).
- [31] T. Sato, D. Uno, and T. S. H. Lee, *Phys. Rev. C* **67**, 065201 (2003).
- [32] K. M. Graczyk, D. Kielczewska, P. Przewlocki, and J. T. Sobczyk, *Phys. Rev. D* **80**, 093001 (2009).
- [33] E. Hernandez, J. Nieves, M. Valverde, and M. J. Vicente Vacas, *Phys. Rev. D* **81**, 085046 (2010).
- [34] K. M. Graczyk, J. Zmuda, and J. T. Sobczyk, *Phys. Rev. D* **90**, 093001 (2014).
- [35] M. R. Schindler, T. Fuchs, J. Gegelia, and S. Scherer, *Phys. Rev. C* **75**, 025202 (2007).
- [36] L. M. Sehgal, in *Proceedings of the International Conference on High Energy Physics*, Geneva, Switzerland, June 27 - July 4, 1979, edited by W. S. Newman and A. Zichichi, Vol. 1, p 98.
- [37] J. Gasser and H. Leutwyler, *Annals Phys.* **158**, 142 (1984).
- [38] C. Patrignani *et al.* [Particle Data Group], *Chin. Phys. C* **40**, 100001 (2016).
- [39] V. A. Andreev *et al.* [MuCap Collaboration], *Phys. Rev. Lett.* **110**, 012504 (2013).
- [40] V. Bernard, N. Kaiser, and U.-G. Meißner, *Phys. Rev. D* **50**, 6899 (1994).

- [41] H. W. Fearing, R. Lewis, N. Mobed, and S. Scherer, *Phys. Rev. D* **56**, 1783 (1997).
- [42] A. R. Edmonds, *Angular momentum in quantum mechanics* (Princeton University Press, Princeton, N. J., 2. ed., 1960).
- [43] J. Gegelia and S. Scherer, *Eur. Phys. J. A* **44**, 425 (2010).
- [44] W. Rarita and J. Schwinger, *Phys. Rev.* **60**, 61 (1941).
- [45] S. Kusaka, *Phys. Rev.* **60**, 61 (1941).
- [46] A. Agadjanov, V. Bernard, U.-G. Meißner, and A. Rusetsky, *Nucl. Phys. B* **886**, 1199 (2014).
- [47] J. Gasser, M. E. Sainio, and A. Švarc, *Nucl. Phys. B* **307**, 779 (1988).
- [48] S. Scherer and M. R. Schindler, *Lect. Notes Phys.* **830**, 1 (2012).
- [49] B. Kubis and U.-G. Meißner, *Nucl. Phys. A* **679**, 698 (2001).
- [50] M. R. Schindler, J. Gegelia, and S. Scherer, *Eur. Phys. J. A* **26**, 1 (2005).
- [51] T. Bauer, J. C. Bernauer, and S. Scherer, *Phys. Rev. C* **86**, 065206 (2012).
- [52] M. Hilt, T. Bauer, S. Scherer, and L. Tiator, *Phys. Rev. C* **97**, 035205 (2018).
- [53] G. Ecker, J. Gasser, H. Leutwyler, A. Pich, and E. de Rafael, *Phys. Lett. B* **223**, 425 (1989).
- [54] G. Ecker, J. Gasser, A. Pich, and E. de Rafael, *Nucl. Phys. B* **321**, 311 (1989).
- [55] N. Fettes, U.-G. Meißner, M. Mojžiš, and S. Steininger, *Annals Phys.* **283**, 273 (2000) Erratum: [*Annals Phys.* **288**, 249 (2001)].
- [56] A. Bodek, S. Avvakumov, R. Bradford, and H. S. Budd, *Eur. Phys. J. C* **53**, 349 (2008).
- [57] R. Gran *et al.* [K2K Collaboration], *Phys. Rev. D* **74**, 052002 (2006).
- [58] V. Lyubushkin *et al.* [NOMAD Collaboration], *Eur. Phys. J. C* **63**, 355 (2009).
- [59] A. A. Aguilar-Arevalo *et al.* [MiniBooNE Collaboration], *Phys. Rev. D* **81**, 092005 (2010).
- [60] L. Fields *et al.* [MINERvA Collaboration], *Phys. Rev. Lett.* **111**, 022501 (2013).
- [61] P. Adamson *et al.* [MINOS Collaboration], *Phys. Rev. D* **91**, 012005 (2015).
- [62] M. Martini, M. Ericson, G. Chanfray, and J. Marteau, *Phys. Rev. C* **80**, 065501 (2009).
- [63] T. Katori and M. Martini, *J. Phys. G* **45**, 013001 (2018).
- [64] B. Bhattacharya, R. J. Hill, and G. Paz, *Phys. Rev. D* **84**, 073006 (2011).
- [65] B. Bhattacharya, G. Paz, and A. J. Tropiano, *Phys. Rev. D* **92**, 113011 (2015).
- [66] A. S. Meyer, M. Betancourt, R. Gran, and R. J. Hill, *Phys. Rev. D* **93**, 113015 (2016).
- [67] R. J. Hill, P. Kammel, W. J. Marciano and A. Sirlin, *Rept. Prog. Phys.* **81**, 096301 (2018).
- [68] L. Alvarez-Ruso, K. M. Graczyk, and E. Saul-Sala, arXiv:1805.00905 [hep-ph] (2018).
- [69] V. Bernard, N. Kaiser, and U.-G. Meißner, *Phys. Rev. Lett.* **69**, 1877 (1992).
- [70] C. E. Carlson and J. L. Poor, *Phys. Rev. D* **34**, 1478 (1986).
- [71] V. Baru, C. Hanhart, M. Hoferichter, B. Kubis, A. Nogga, and D. R. Phillips, *Nucl. Phys. A* **872**, 69 (2011).
- [72] Y. Ünal, A. Küçükarslan, and S. Scherer, in preparation.
- [73] M. L. Goldberger and S. B. Treiman, *Phys. Rev.* **110**, 1178 (1958).
- [74] Y. Nambu, *Phys. Rev. Lett.* **4**, 380 (1960).